Biol Trace Elem Res (2016) 170:309–319
DOI 10.1007/s12011-015-0467-4

Time and Concentration-Dependent Therapeutic Potential of Silver Nanoparticles in Cervical Carcinoma Cells

Muthuraman Pandurangan[1] · Gansukh Enkhtaivan[1] · Baskar Venkitasamy[2] · Bhupendra Mistry[1] · Rafi Noorzai[1] · Bong Yeon Jin[1] · Doo Hwan Kim[1]

Received: 5 June 2015 / Accepted: 3 August 2015 / Published online: 15 August 2015

Abstract Silver nanoparticles (AgNPs) have well-known anti-bacterial properties and have been widely used in daily life as various medical and general products. There is limited information available on the cytotoxicity of AgNPs. Therefore, the present study aimed to investigate the cytotoxicity of AgNPs in HeLa cells. Cytotoxicity and apoptosis have been observed in the AgNPs treated in the HeLa cells. Sulphorhodamine-B assay (SRB assay) showed the cytotoxic effect in the AgNP-treated HeLa cells. Inverted microscope, fluorescence microscope, and confocal laser scanning microscope (CLSM) analyses showed the apoptosis-induced morphological changes such as rounding in shape, nuclear fragmentation, cytoplasm reduction, loss of adhesion, and reduced cell volume. Necrosis and apoptosis were observed in the AgNP-treated HeLa cells by DNA fragmentation study. Mitochondria-derived reactive oxygen species (ROS) have increased in AgNP-treated HeLa cells. Up-regulation of messenger RNA (mRNA) expression of p53, bax, and caspase 3 were found in AgNP-treated HeLa cells. Caspase 3 enzyme activity was found to increase in AgNP-treated HeLa cells. The AgNPs showed the right cytotoxic effect in cervical carcinoma cells. Our results suggest that metal-based nanoparticles might be a potential candidate for the treatment of cervical cancer.

Keywords AgNPs · HeLa cells · Fluorescence microscope · Confocal microscope · SRB · Apoptosis

Electronic supplementary material The online version of this article (doi:10.1007/s12011-015-0467-4) contains supplementary material, which is available to authorized users.

✉ Bong Yeon Jin
byj@sunbio2.com

✉ Doo Hwan Kim
frenzram1980@gmail.com

[1] Department of Bioresources and Food Science, Konkuk University, Seoul, South Korea

[2] Department of Molecular Biotechnology, Konkuk University, Seoul, South Korea

Introduction

Apoptosis is a highly regulated process of programmed cell death in which cells will undergo a tightly regulated program that plays a critical role in the normal and pathological process [1]. Cellular and nuclear shrinkage, nuclear fragmentation, condensation, the formation of apoptotic bodies, and cellular budding are critical apoptotic features. Nucleus and cytoplasm are condensed to produce a membrane-bound apoptotic bodies that are phagocytized by macrophages [2]. Uncontrolled proliferation and loss of apoptosis are major factors for tumor formation. A compound that prevents the proliferation of tumor cells by the induction of apoptosis has been considered a potential anti-tumor compound [3].

Silver nanoparticles (AgNPs) have been used as nanomaterials due to its anti-bacterial properties. AgNPs have been commonly utilized in the medical field such as coatings for wound dressings, implants, bone prostheses, and surgical instruments [4–6]. Nanoparticles elicit a greater biological response than microparticles [7], and it could affect cellular activity significantly [8]. Lynch et al. [9] have reported that the cytotoxicity of nanoparticles due to its smaller size, high number per given mass, large specific surface area, and generation of reactive oxygen species ROS. AgNP coatings have been widely used in textile industries for the manufacture of clothes and socks [10–11]. AgNPs have been commercialized as deodorants, room sprays, water cleaners, wall paints, and laundry detergents. Therefore,

exposure of AgNP could occur to these consumers and laborers at the manufacturing site. Ionic silver is highly toxic to bacteria. Due to adsorption to the bacterial cell wall, de-activation of enzymes and ROS production [12–15]. AgNPs inhibits bacterial growth through attachment to cell membranes, changes of membrane permeability, and accumulation of intracellular ROS [16–18].

Several studies have reported on the biological effects of AgNPs in mammalian cells. However, the exact mechanism of AgNPs is not yet completely understood. A selection of HeLa cells based on being monocytic lineage could mimic local immune responses [19], and cervical carcinoma is one of the most common neoplastic diseases affecting women [20]. Chemotherapy, radiotherapy, and surgery could damage the cancer cells and some healthy cells in the body. These treatments are highly expensive and produce severe side effects including bone marrow problems, hair loss, nausea, and fatigue. Therefore, development of novel and efficient anti-cancer drugs, which, also, should overcome resistance, has become a significant issue.

We evaluated the toxicity of AgNPs and expression levels of several apoptotic-related markers in the HeLa cells. SRB assay investigated the cytotoxicity of AgNPs on cells. Apoptotic changes were observed by an inverted microscope, fluorescence microscope, and confocal laser scanning microscope (CLSM). DNA fragmentation students and quantitative polymerase chain reaction (qPCR) were carried out on apoptosis-related gene messenger RNA (mRNA) expressions. Caspase 3 enzyme activity and ROS levels were also determined.

Materials and Methods

Materials

AgNPs (10 nm (TEM), cat no. 730,785, Sigma-Aldrich), dimethyl sulphoxide (DMSO), and sulforhodamine B (SRB) were purchased from Sigma. DMEM, fetal bovine serum (FBS), penicillin-streptomycin, and trypsin-EDTA were obtained from Welgene (Daegu, South Korea). Acridine orange (AO), ethidium bromide (EB), and 2′,7′-dichlorofluorescin diacetate (DCFH-DA) were purchased from Santa Cruz Biotechnology, Inc. (Delaware Avenue, California, USA). Primers have been obtained from Macrogen Inc. (South Korea).

Cell Culture

HeLa cells were purchased from the Korean Cell Line Bank (South Korea). Cells were kept in the growth medium supplemented with 10 % FBS and 1 % antibiotics (penicillin-streptomycin). The cells were grown in a CO_2 incubator at 37 °C and 5 % CO_2.

SRB Assay

A 96-well plate was used for the culturing cells and allowed to adhere for 24 h at 37 °C. Cells were treated with AgNPs at different concentrations (0.001, 0.01, 0.02, 0.04, 0.08, and 0.16 mg/ml) for 48 and 72 h. The cytotoxic effect of HeLa cells was measured by the SRB assay [21].

Inverted Microscope

A 6-well plate was used for the culturing HeLa cells at a density of 2×10^5 cells/well. The cells were treated with AgNPs of different concentrations (0.01, 0.02, and 0.04 mg/ml) for 48 and 72 h after 24 h of adherence. After treatments, the morphology of cells was examined by an inverted microscope (Nikon, Eclipse, 80i, Melville, NY 11747-3064, USA).

Fluorescence Microscope

A 6-well plate was used for the used for the culturing cells at a density of 2×10^4 cells/well. The cells were treated with AgNPs of different concentrations (0.01, 0.02, and 0.04 mg/ml) for 48 and 72 h. Cells were examined with fluorescence microscope (Axiovert 2000, Carl Zeiss, Germany) [22].

CLSM

HeLa cells were seeded in the confocal dish. After 24 h of adherence, the cells were treated with AgNP of different concentrations (0.01, 0.02, and 0.04 mg/ml). After 48 and 72 h, cells were washed thrice with PBS and stained with AO (20 μg/ml) for 5 min. Cells were viewed immediately under CLSM ($1X81^R$ Motorized Inverted Microscope, Olympus [22].

DNA Fragmentation Study

A 6-well plate was used for the culturing of HeLa cells. The cells were treated with AgNPs of different concentrations (0.01, 0.02, and 0.04 mg/ml) for 48 and 72 h. A DNA was isolated from the cells using an extraction method [23]).The evaluation of the size range of the fragmented DNA was performed by electrophoresis using a 1.5 % agarose gel in Tris/borate/EDTA (TBE) buffer at a constant of 100 mA for 120 min.

qPCR

Total RNA was isolated from the control and AgNP-treated samples [24]. Primers specific for p53 (forward:5′-TAACAG TTCCTGCATGGGCGGC-3′, reverse: 5′-AGGACAGGC ACAAACACGCACC-3′), bax (forward:5′-TGG AGCTGC

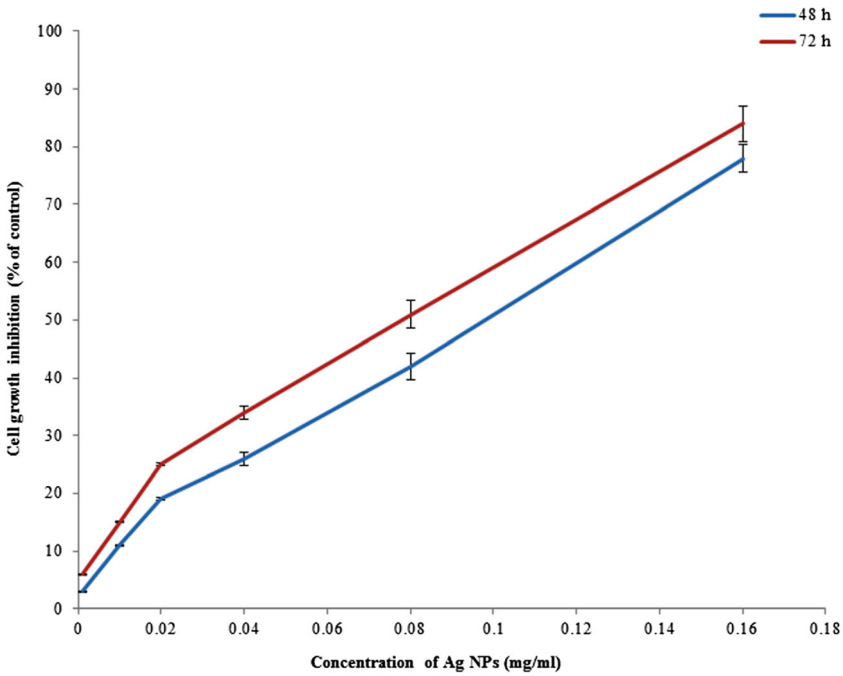

Fig. 1 Cytotoxic effect of AgNPs in HeLa cells by SRB assay at 48 and 72 h. Results have presented as a percentage of growth inhibition compared with the control. The percentage of growth inhibition was calculated as follows: Growth inhibition (%): (control − sample/control)×100. Values are shown as means ± SEM

AGAGGATGATTG-3′, reverse: 5′-GAAGTTGCCGTCA GAAAACATG-3′), caspase 3 (forward: 5′-TTAATAAAGGT ATCCATGGAGAACACT-3′, reverse: 5′-TTAGTGATAA AAATAGAGTTCTTTTGTGAG-3′) and a housekeeping gene GAPDH (forward: 5′-GGTCACCAGGGCTGCTTTT-3′, reverse: 5′-ATCTCGCTCCTGGAAGATGGT-3′) were used in this study. The relative ratios were determined based on the $2^{-\Delta\Delta}{}_{CT}$ method (Pfaffl, 2001). PCR was monitored using the CFX96™ Real-Time System (Bio-Rad).

Caspase Activity Assay

HeLa cells were seeded in the culture dish. After 24 h adherence, the cells were treated with AgNPs of different concentrations

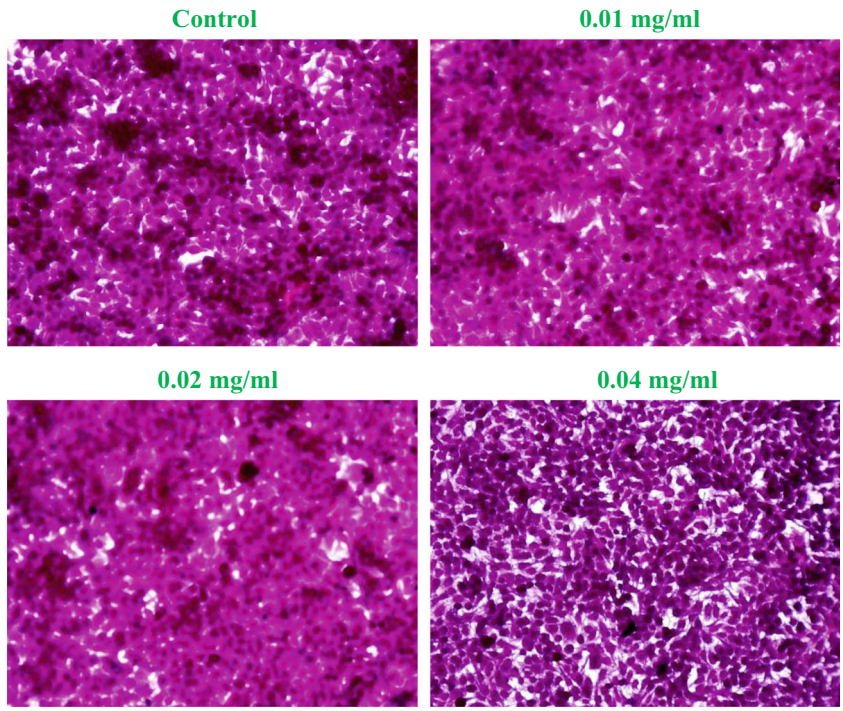

Fig. 2 Cytotoxic effect of AgNPs in HeLa cells by SRB assay at 48 h. The morphology of cells were observed by an inverted microscope (×40). The representative images were obtained from three independent experiments

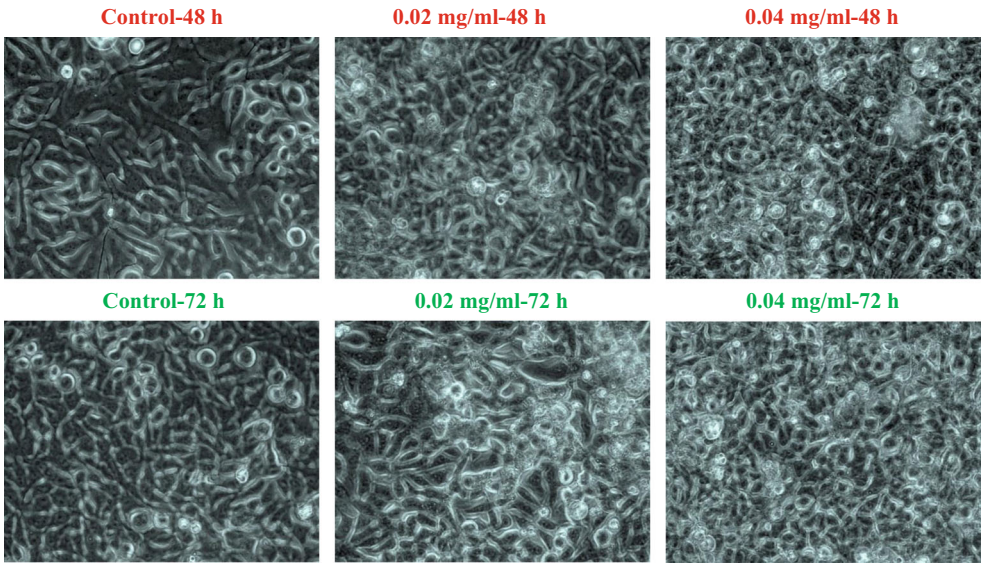

Fig. 3 The morphological observation by an inverted microscope following AgNPs exposure at 48 and 72 h. The representative images were obtained from three independent experiments

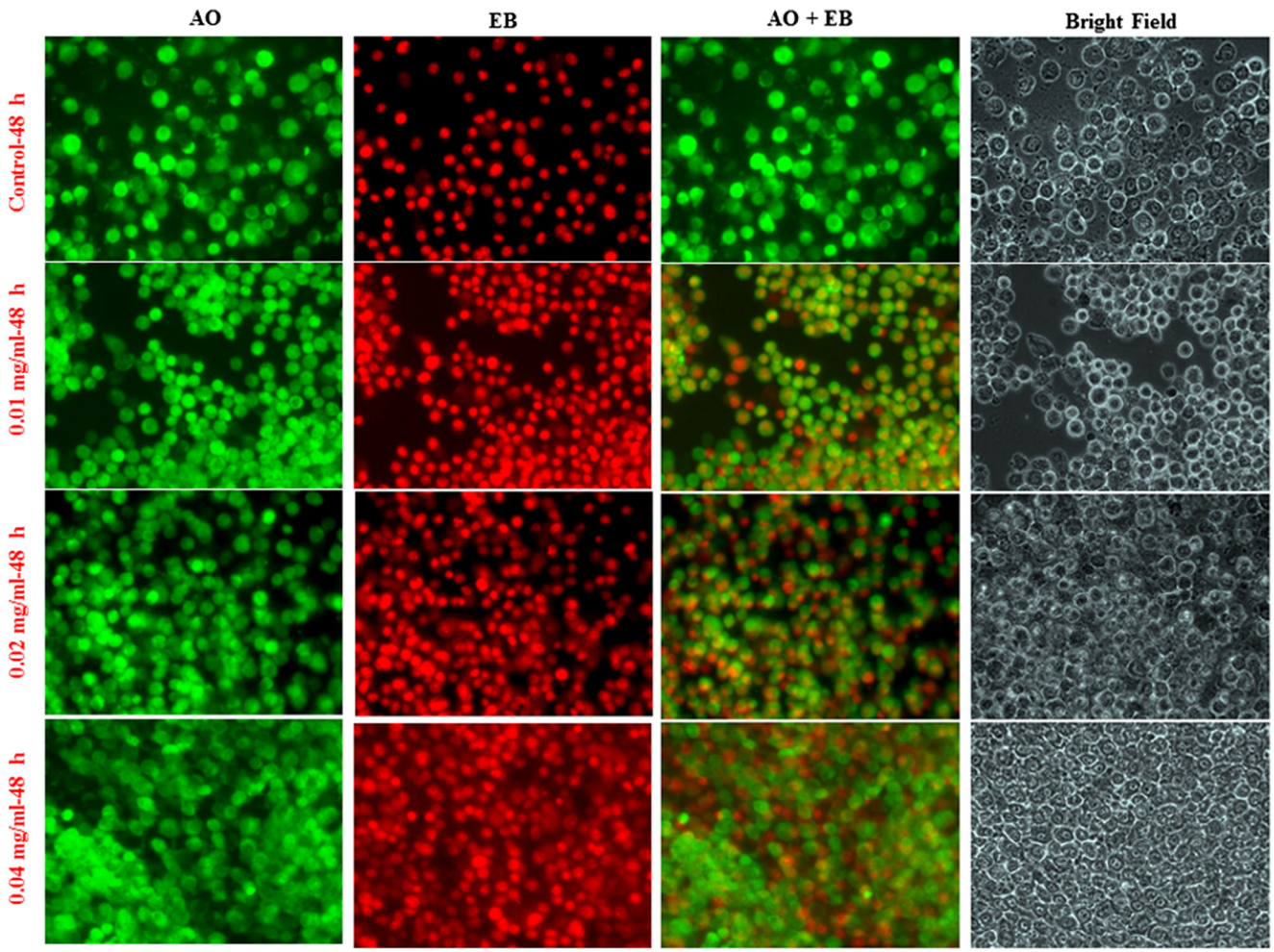

Fig. 4 The morphological observation with AO/EB double staining by a fluorescence microscope (×40). HeLa cells were seeded in 6-well plates, and over 24 of adherence, cells were treated with AgNPs (0.01, 0.02, and 0.04 mg/ml) for 48 h. The representative images were obtained from three independent experiments

(0.01, 0.02, and 0.04 mg/ml). After 48 and 72 h, caspase 3 enzyme activity was measured based on the method of Muthuraman [25].

Determination of ROS Production

ROS was determined using a fluorescent probe, 2,7, dichlorodihydrofluorescein diacetate (DCFH-DA) [22]. Cells were seeded in 96-well plates in growth medium at a cell density of 5000 cells/well. The cells were treated with AgNPs for 48 and 72 h. The medium was removed, and the cells were incubated with 5 μM of DCFH-DA in the growth medium for 30 min at 37 °C and 5 % CO_2. The fluorescence was measured using a fluorescent plate reader, and images were taken using fluorescence microscope (Axiovert 2000, Carl Zeiss, Germany).

Statistical Analysis

Values are expressed as means ± SEM. The difference between control and AgNP-treated cells was evaluated using Student's *t* test. A *p* value of less than 0.05 was considered statistically significant.

Results

Cytotoxicity of AgNP

AgNPs showed an apparent cytotoxic effect on HeLa cells, and clear concentration-response relationship was observed (Fig. 1). Stained cells were photographed at 48 h (Fig. 2) and 72 h (Fig. S1). However, 0.08 and 0.16 mg/ml AgNP could inhibit the growth of HeLa cells. This result suggested that 0.08 and 0.16 mg/ml AgNP could be toxic to normal cells. Therefore 0.01, 0.02, and 0.04 mg/ml of AgNP was used for further study.

Observation by Inverted Microscope

Inverted microscope could be used to observe the HeLa cell shape and its morphological changes. Control cells were

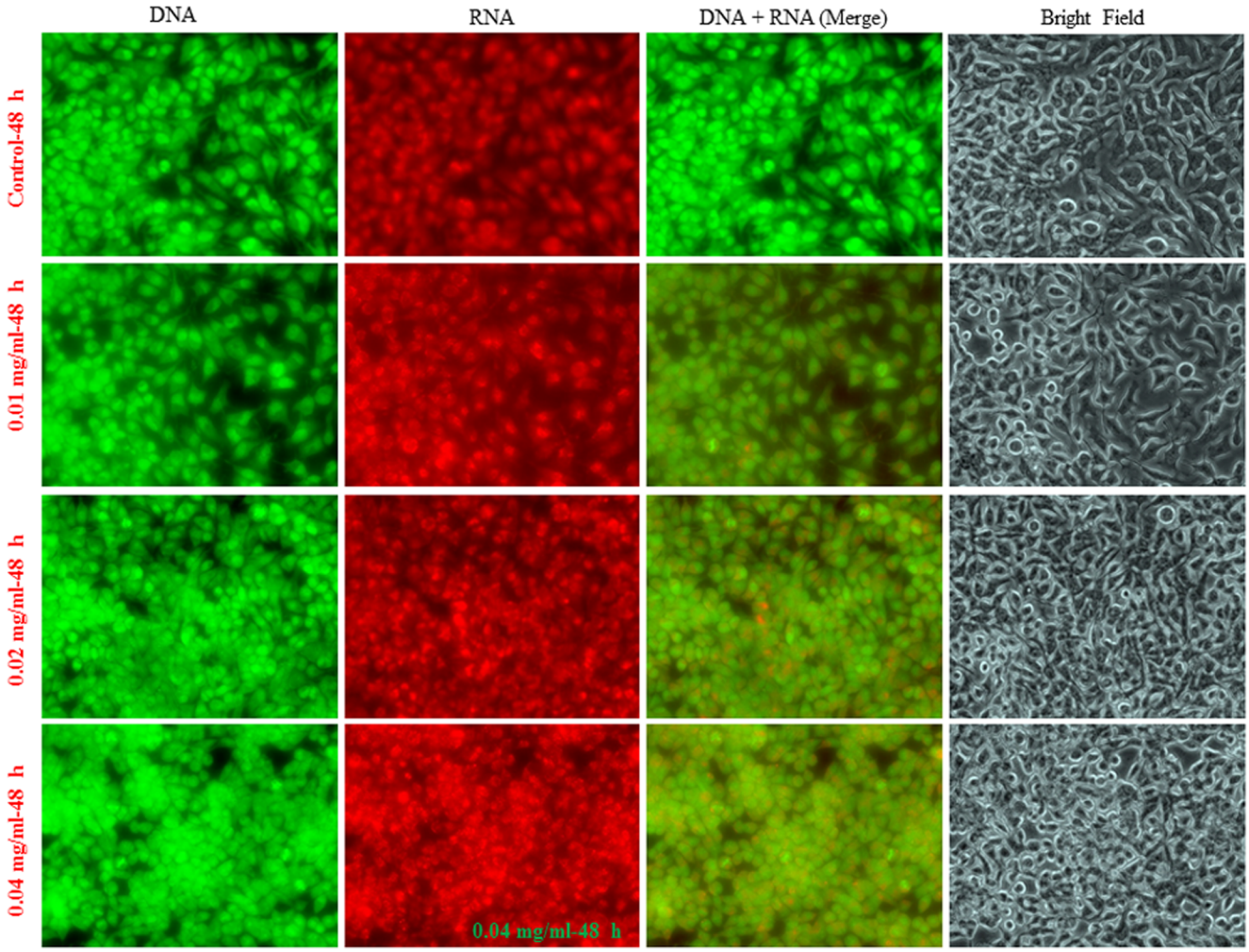

Fig. 5 Morphological observation of HeLa cells by CLSM (×40). HeLa cells were grown on the cover glass confocal dish. After 24 h of adherence, cells were treated with AgNP (0.01, 0.02, and 0.04 mg/ml) for 48 h. The representative images were obtained from three independent experiments

regular polygonal form and short cell antennas were seen. AgNPs treated HeLa cells showed significant morphological changes such as sporadic distribution, loss of adherence and rounding. There is clear concentration-dependent response relationship was observed (Fig. 3).

Observation by Fluorescence Microscope

Fluorescence microscopy was carried out to determine whether the cytotoxic effect of AgNP was related to the induction of apoptosis, morphological features of cell death. This method combines the dual uptake of fluorescent DNA-binding dyes AO and EB. Control cells have no apparent morphological changes. Viable cells possess a uniform bright green nucleus. Early apoptotic cells show bright green areas of fragmented chromatin in the nucleus, and necrotic cells show an identical bright orange nucleus. However, HeLa cells exposed to AgNP for 48 and 72 h exhibited fragmented and condensed chromatin, fragmented nuclei, and appearance of apoptotic bodies. The results were correlated with clear concentration-dependent response relationships (Fig. 4; Fig. S2).

Observation by CLSM

CLSM has been widely applied to investigate morphological studies of apoptosis and apoptotic DNA fragmentation [26]. AO can interact with DNA (green) and RNA (red). Control HeLa cells have bigger and smoother nucleus than AgNP-treated cells. The morphological changes including rounding, compact granular masses in the nucleus, and reduced nuclear volume were seen following treatment. The appearance of bright green nucleus suggests the induction of apoptosis in AgNP-treated cells. Chromatin and nuclear membrane were aggregated, and condensed cytoplasm was also observed in the AgNP-treated cells. The level of morphological changes is in a concentration-dependent response relationship (Fig. 5; Fig. S3).

Quantification of Apoptotic Cells

AgNPs induced apoptosis in HeLa cells and are investigated by the fluorescence and confocal microscopes over 48 and 72 h. The hundred cells were counted for control and each concentration point. The percentage of apoptotic cells was found to be 42, 51, and 55 % in 0.01, 0.02, and 0.04 mg/ml AgNP-treated samples by fluorescence microscope, whereas it was 54, 60, and 62 %, respectively. The percentage of apoptotic cells was found to be 61, 62, and 65 % in 0.01, 0.02, and 0.04 mg/ml AgNP-treated samples by confocal microscope, whereas it was 67, 70, and 71 %, respectively. The percentage of apoptotic cells showed slight concentration-response relationships (Table 1).

Table 1 Induction of apoptosis in HeLa cells by AgNPs and observed by the fluorescence and confocal microscopes over 48 and 72 h

Concentrations (mg/ml)	Apoptotic cells (%)			
	Fluorescence study		Confocal study	
	48 h	72 h	48 h	72
Control	0 ± 0	0 ± 0	0 ± 0	0 ± 0
0.01	42 ± 2*	54 ± 3*	61 ± 3*	67 ± 4*
0.02	51 ± 4*	60 ± 2*	62 ± 3*	70 ± 2*
0.04	55 ± 3*	62 ± 2*	65 ± 5*	71 ± 4*

A hundred HeLa cells were counted for each concentration. The percentage of apoptotic cells were calculated from the following formula. Apoptotic cells (%): (number of apoptotic cells/total number of cells)× 100. Values were expressed as means ± SD of three independent experiments

$p < 0.05$

AgNP-Induced DNA Fragmentation

DNA fragmentation is a hallmark of apoptosis. Cell death can be defined as morphological and biochemical feature changes that differentiate it from other forms of cell death. An endonuclease cleaves the DNA into small fragments. Cells were

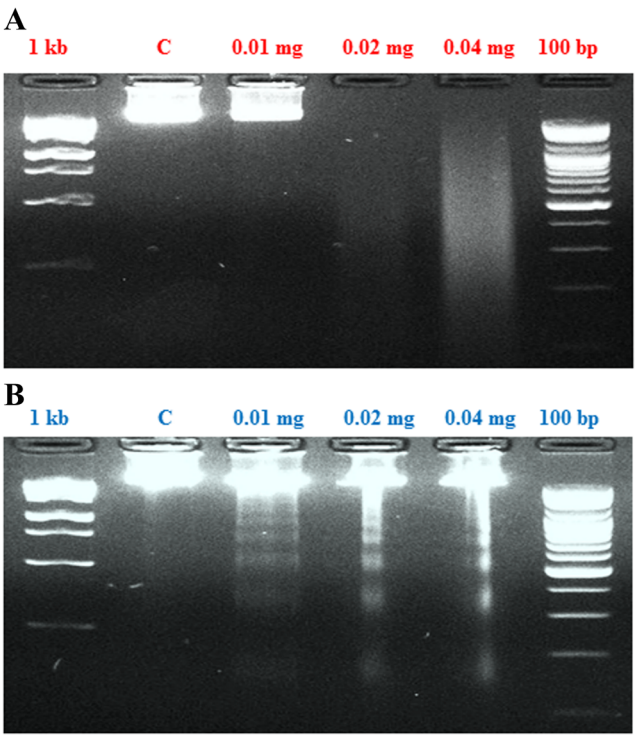

Fig. 6 DNA fragmentation analysis by classical agarose gel electrophoresis. HeLa cells were grown in 6-well plates and allowed for the adherence for 24 h. Cells were treated with AgNPs (0.01, 0.02, and 0.04 mg/ml) for 48 and 72 h. At the end of treatments, DNA was isolated from the cells using extraction method. The evaluation of the size range of the fragmented DNA was performed by electrophoresis using a 1.5 % agarose gel in TBE buffer at a constant of 100 mA for 120 min. The representative images were obtained from three independent experiments

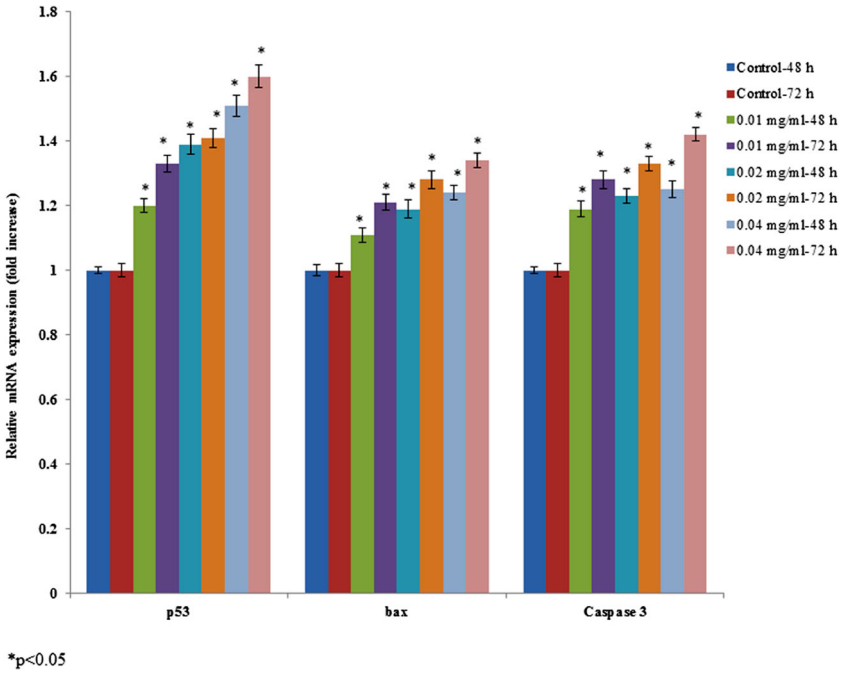

Fig. 7 mRNA expression of apoptotic p53, bax, and caspase 3 genes by qPCR. HeLa cells were grown in a T-25 flask and allowed for adherence for 24 h. Cells were treated with AgNPs (0.01, 0.02, and 0.04 mg/ml) for 48 and 72 h. Values are shown as means ± SEM.

seeded at a density of 2.5×10^4 cells/well. Multiple oligomers and smear did not appear in the control cells, whereas smear and various bands were appearing in treated cells in a concentration-dependent manner (Fig. 6).

AgNP-Induced Apoptotic Marker Gene Expression

To further confirm necrosis and apoptosis, we constituted apoptotic marker gene expression by qPCR. HeLa cells exposed to different concentrations of AgNPs (0.01, 0.02, and 0.04 mg/ml) for 48 and 72 h showed significant changes in the mRNA expression of *p53*, *bax*, and *caspase 3* gene. The mRNA expression level of p53, bax, and caspase 3 were significantly up-regulated in AgNP-treated cells compared with controls. The mRNA expression of p53 was increased (0.2-, 0.39-, and 0.51-fold) at 48 h and (0.33-, 0.41-, and 0.6-fold) at 72 h, following 0.01, 0.02, and 0.04 mg/ml of AgNP treatments, respectively. The mRNA expression of bax was increased (0.11-, 0.19-, and 0.24-fold) at 48 h and (0.21-, 0.28-, and 0.34-fold) at 72 h, following 0.01, 0.02, and 0.04 mg/ml of AgNP treatments,

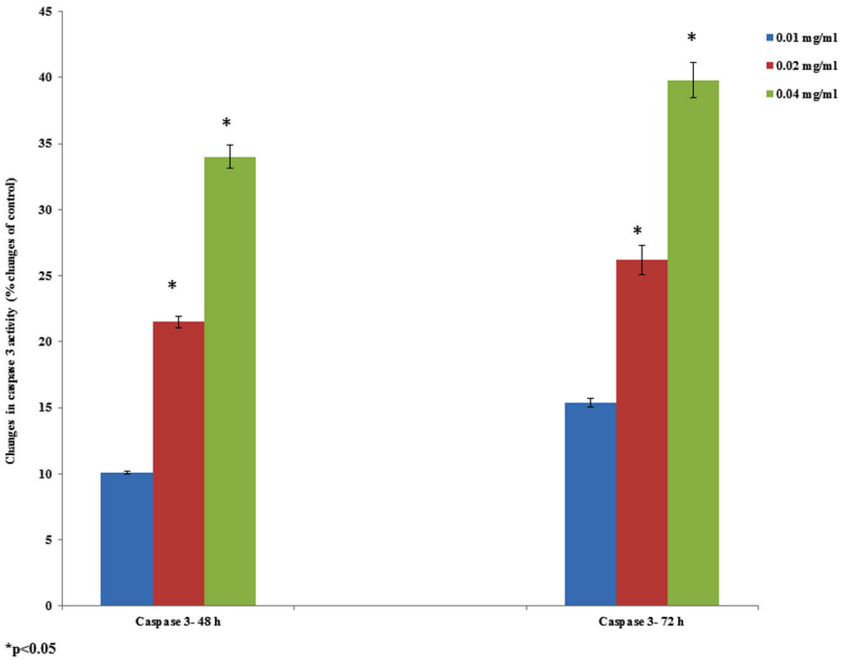

Fig. 8 Changes in caspase 3 enzyme activity. HeLa cells were grown in a T-75 flask and allowed for adherence for 24 h. Cells were treated with AgNPs (0.01, 0.02, and 0.04 mg/ml) for 48 and 72 h. At the end of treatments, cells were removed and activity was determined as mentioned in the "Materials and Methods." Values have shown as means ± SEM

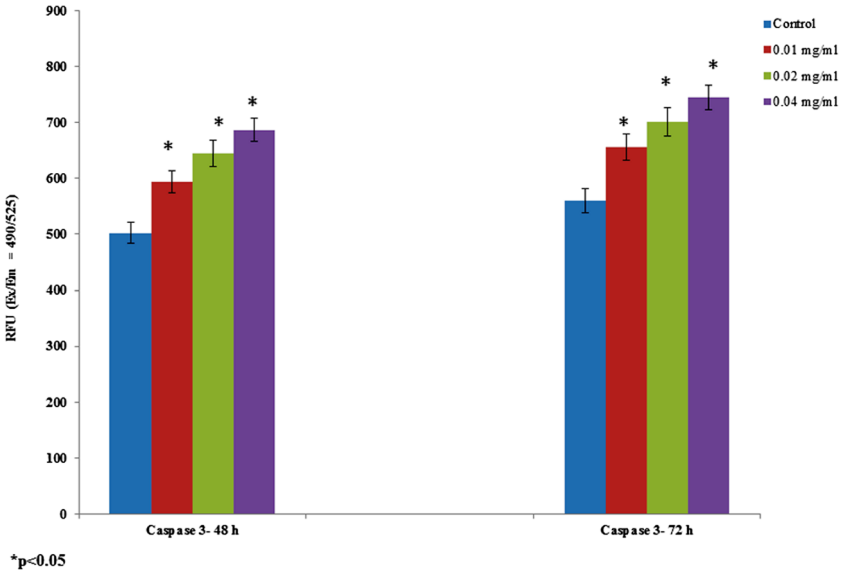

Fig. 9 Changes in fluorescence intensity. Cells were treated with AgNPs (0.01, 0.02, and 0.04 mg/ml) for 48 and 72 h. Cells were treated with dye as mentioned in the "Materials and Methods." Values are shown as means ± SEM

respectively. The mRNA expression of caspase 3 was increased (0.19-, 0.23-, and 0.25-fold) at 48 h and (0.28-, 0.33-, and 0.42-fold) at 72 h, following 0.01, 0.02, and 0.04 mg/ml of AgNP treatments, respectively (Fig. 7).

AgNP-Induced Effect on Caspase-3 Activity

Caspases are cysteine proteases and act as central executioners of the apoptotic pathway [27]. Caspase 3 activity was increased 10.1, 21.5, and 34 % in AgNP-treated cells at 48 h, following 0.01, 0.02, and 0.04 mg/ml of treatments, respectively, whereas 15.4, 26.2, and 39.8 % at 72 h of treatment (Fig. 8).

AgNP-Induced Intracellular ROS Production

The fluorescent probe DCFH-DA determined the intracellular ROS generation. The fluorescence study indicated that the green fluorescence intensity of DCF was enhanced in the AgNP-treated cells compared with the control cells. These results indicated that the AgNPs induced intracellular ROS generation in a dose-dependent manner (Figs. 9, 10, and 11; Fig. S4).

Discussion

Nanoparticles attracted several researchers due to their unique properties such as electronic, optical, mechanical, catalytic,

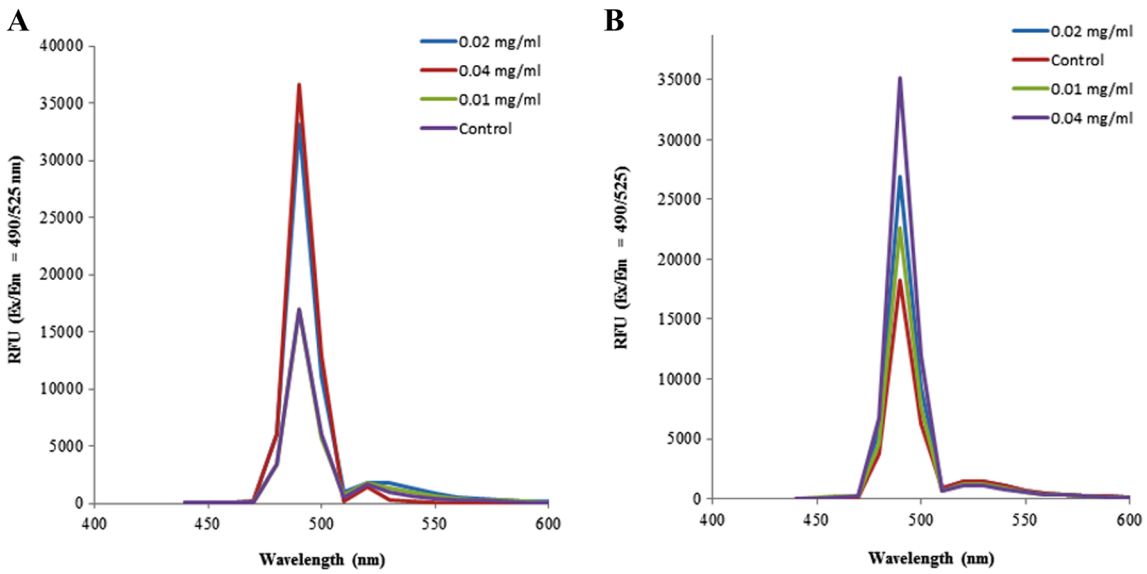

Fig. 10 Changes in fluorescence intensity. Cells were treated with AgNPs (0.01, 0.02, and 0.04 mg/ml) for 48 and 72 h. Cells were stained with dye, and spectrum was taken for 48-h treatment (**a**) and 72-h treatment (**b**)

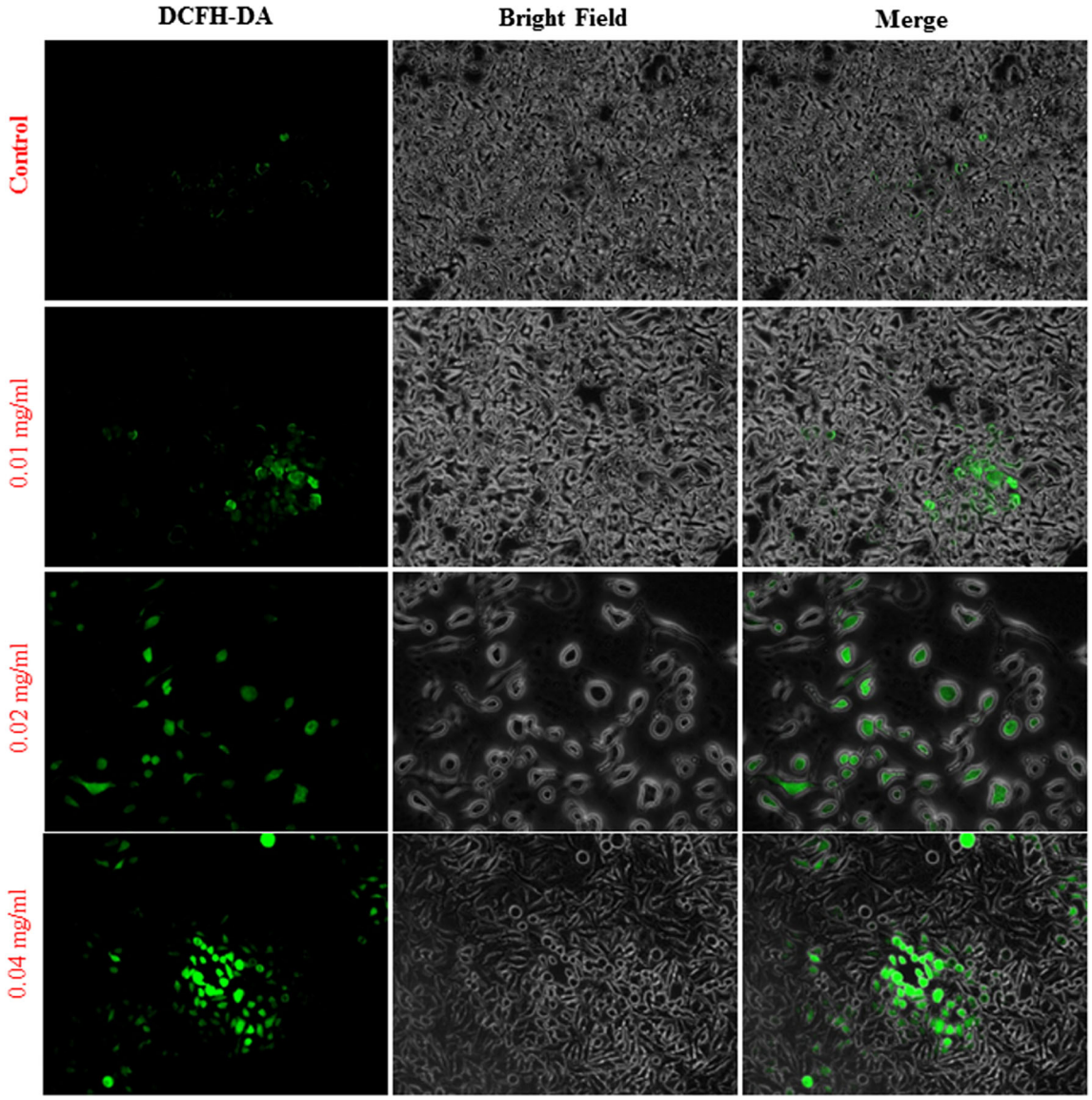

Fig. 11 Changes in fluorescence intensity. HeLa cells were grown in 6-well plates and allowed for the adherence for 24 h. Cells were treated with AgNPs (0.01, 0.02, and 0.04 mg/ml) for 48 h. Cells were stained with dye, and images were taken using fluorescence microscope

and biological properties [28–29]. The metal nanoparticles, AgNPs, are one of the promising nanoparticles used in nanomedicine because of their unique properties. AgNPs are widely used in topical ointments to prevent infection against burn and open wounds [30] and in anti-microbial [31], anti-fungal [32], anti-inflammatory [33], anti-viral [34], anti-angiogenesis [35], and anti-platelet activity [36].

Cancer is one of the leading causes of deaths due to its profound complex in nature. Cervical cancer is the second most common cancer in females. Cervical cancer is due to the infection with the human papilloma virus [37]. Chemotherapy, radiotherapy, and surgery could damage the cancer cells and some healthy cells in the body. These treatments are highly expensive and produce severe side effects including bone marrow problems, hair loss, nausea, emesis, and fatigue [38]. Therefore, development of novel and efficient anti-cancer drugs, which, also, should overcome resistance, has become a significant issue.

The tumor cell apoptosis induction is an essential mechanism of anti-cancer compound [3]. Apoptosis process has been characterized by the morphological and biochemical changes, and apoptosis of different cells in the same tissue do not occur at the same time. The morphological observation is critical for apoptosis study in the early stage because observations can see DNA multiplies after initiation of apoptosis. The apoptotic effect of AgNPs was reported using mouse NIH3T 3 cells [39]. Formation of DNA fragments is regarded as a biochemical hallmark of apoptosis [40]. Classical methods to study the cell death are morphological and biochemical feature changes that differ from other forms of cell

death. An endonuclease enzyme cleaves the DNA into small fragments. In agreement with the above finding, our results also showed DNA fragmentation in a dose-dependent manner in the HeLa cells.

The gene *p53* triggers cell-cycle arrest to provide time for the repayment and self-medicated apoptosis during cellular stress [41]. The role of p53 is to up-regulate the expression of bax gene. AgNPs increased caspase 3 mRNA expression and activity in a concentration-dependent manner. The up-regulated caspase-3 activates auto-catalysis, cleaving other members of the caspase family leading to irreversible apoptosis [42]. Apoptosis-related genes were altered in the liver of AgNP-fed mice [43]. Apoptosis process could occur in response to oxidative stress [44]. AgNP-mediated generation of ROS was reported in an in vitro study [39]. In agreement with this finding, ROS level was up-regulated in our study due to oxidative stress. These results indicate that apoptosis induction by AgNPs may be carried out by ROS generation.

Conclusion

The AgNPs showed the right cytotoxic effect in cervical carcinoma cells. Our results suggest that metal-based nanoparticles might be a potential candidate for the treatment of cervical cancer. Taking all these data together, it can be concluded that the AgNP could exert cytotoxicity on HeLa cell through the apoptotic pathway.

Acknowledgments This work was supported by the KU Research Professor Program of Konkuk University, Seoul, South Korea.

Conflict of Interest The authors declare no conflict of interest

References

1. Reed JC (2001) Apoptosis-regulating proteins as targets for drug discovery. Trends Mol Med 7:314–319
2. Darzynkiewicz Z, Juan G, Li X, Gorczyca W, Murakami T, Traganos F (1997) Cytometry in cell necrobiology: analysis of apoptosis and accidental cell death (necrosis). Cytometry 27:1–20
3. Frankfurt OS, Krishan A (2003) Apoptosis-based drug screening and detection of selective toxicity to cancer cells. Anticancer Drugs 14:555–561
4. Cohen MS, Stern JM, Vanni AJ, Kelley RS, Baumgart E, Field D, Libertino JA, Summerhayes IC (2007) In vitro analysis of a nanocrystalline silver-coated surgical mesh. Surg Infect (Larchmt) 8: 397–403
5. Fu J, Ji J, Fan D, Shen J (2006) Construction of antibacterial multilayer films containing nanosilver via layer-by-layer assembly of heparin and chitosansilver ions complex. J Biomed Mater Res A 79:665–674
6. Xu X, Yang Q, Bai J, Lu T, Li Y, Jing X (2008) Fabrication of biodegradable electrospun poly (L-lactide-co-glycolide) fibers with antimicrobial nanosilver particles. J Nanosci Nanotechnol 8:5066–5070
7. Borm PJ, Robbins D, Haubold S, Kuhlbusch T, Fissan H, Donaldson K, Schins R, Stone V, Kreyling W, Lademann J, Krutmann J, Warheit D, Oberdorster E (2006) The potential risks of nanomaterials: a review carried out for ECETOC. Part Fiber Toxicolo 3:11
8. Sayes CM, Wahi R, Kurian PA, Liu Y, West JL, Ausman KD, Warheit DB, Colvin VL (2006) Correlating nanoscale titania structure with toxicity: a cytotoxicity and inflammatory response study with human dermal fibroblasts and human lung epithelial cells. Toxicol Sci 92:174–185
9. Lynch I, Dawson KA, Linse S (2006) Detecting cryptic epitopes created by nanoparticles. Sci STKE 327:14
10. Benn TM, Westerhoff P (2008) Nanoparticle silver released into water from commercially available sock fabrics. Environ Sci Technol 42:4133–4139
11. Vigneshwaran N, Kathe AA, Varadarajan PV, Nachane RP, Balasubramanya RH (2007) Functional finishing of cotton fabrics using silver nanoparticles. J. Nanosci Nanotechnol 7:1893–1897
12. Matsumura Y, Yoshikata K, Kunisaki S, Tsuchido T (2003) Mode of bactericidal action of silver zeolite and its comparison with that of silver nitrate. Appl Environ Microbiol 69:4278–4281
13. Navarro E, Piccapietra F, Wagner B, Marconi F, Kaegi R, Odzak N, Sigg L, Behra R (2008) Toxicity of silver nanoparticles to Chlamydomonas reinhardtii. Environ Sci Technol 42:8959–8964
14. Sambhy V, MacBride MM, Peterson BR, Sen A (2006) Silver bromide nanoparticle/polymer composites: dual action tunable antimicrobial materials. J Am Chem Soc 128:9798–9808
15. Slawson RM, Van Dyke MI, Lee H, Trevors JT (1992) Germanium and silver resistance, accumulation, and toxicity in microorganisms. Plasmid 27:72–79
16. Lok CN, Ho CM, Chen R, He QY, Yu WY, Sun. H, Tam PK, Chiu JF, Che CM (2006) Proteomic analysis of the mode of antibacterial action of silver nanoparticles. J Proteome Res 5: 916–924.
17. Nel A, Xia T, Madler L, Li N (2006) Toxic potential of materials at the nano level. Science 311:622–627
18. Sondi I, Salopek-Sondi B (2004) Silver nanoparticles as antimicrobial agent: a case study on E. coli as a model for Gram-negative bacteria. J Colloid Interface Sci 275:177–182
19. Cimpan MR, Cressey LI, Skaug N, Halstensen A, Lie SA, Gjertsen BT, Matre R (2000) Patterns of cell death induced by eluates from denture base acrylic resins in U-937 human monoblastoid cells. Eur J Oral Sci 108:59–69
20. Franco EL, Schlecht NF, Saslow D (2003) The epidemiology of cervical cancer. Cancer J 9:348–359
21. Muthuraman P, Enkhtaivan G, Bhupendra M, Chandrasekaran M, Rafi N, Kim DH (2015) Investigation of role of aspartame on apoptosis process in Hela cells. Saudi Journal of Biological Sciences. doi:10.1016/j.sjbs.2015.06.001
22. Muthuraman P, Kim DH, Muthuviveganandavel V, Vikramathithan J, Ravikumar S (2015) Differential bio-potential of ZnS nanoparticles to normal MDCK cells and cervical carcinoma HeLa cells. Journal of Nanoscience and Nanotechnology 15:1–8
23. Merante F, Raha S, Ling M (1998) Isolation of total cellular DNA from tissues and cultured cells. Molecular biomethods handbook. 9–16.
24. Muthuraman P, Muthuviveganandavel V, Kim DH (2015) Cytotoxicity of zinc oxide nanoparticles on antioxidant enzyme activities and mRNA expression in the cocultured C2C12 and 3T3-L1 Cells. Applied Biochemistry and Biotechnology 175(3): 1270–1280
25. Muthuraman P (2014) Effect of cortisol on caspases in the co-cultured C2C12 and 3T3-L1 cells. Applied Biochemistry and Biotechnology 173(4):980–988
26. Tattona NA, Rideout HJ (1999) Confocal microscopy as a tool to examine DNA fragmentation, chromatin condensation and other

apoptotic changes in Parkinson's disease. Parkinsonism and Related Disorders 5:179–186
27. Hengartner MO (2000) The biochemistry of apoptosis. Nature 407: 770–776
28. Muthuraman P, Kim DH (2015) In vitro toxicity of zinc oxide nanoparticles: a review. Journal of Nanoparticle Research 17:158
29. Muthuraman P, Ramkumar K, Kim DH (2014) Analysis of the dose-dependent effect of zinc oxide nanoparticles on the oxidative stress and antioxidant enzyme activity in adipocytes. Applied Biochemistry and Biotechnology 174(8):2851–2863
30. Ip M, Lui SL, Poon VKM, Lung I, Burd A (2006) Antimicrobial activities of silver dressings: an in vitro comparison. J Med Microbiol 55:59–63
31. Sriram MI, Mani Kanth SB, Kalishwaralal K, Gurunathan S (2010) Antitumor activity of silver nanoparticles in Dalton's lymphoma ascites tumor model. Int J Nanomed 5:753–762
32. Medina-Ramirez I, Bashir S, Luo Z, Liu JL (2009) Green synthesis and characterization of polymer stabilized silver nanoparticles. Coll Sur B: Biоint 73:185–191
33. Panacek A, Kolar M, Vecerova R, Prucek R, Soukupova J, Krystof V, Hamal P, Zboril R, Kvitek L (2009) Antifungal activity of silver nanoparticles against *Candida* spp. Biomat 30:6333–6340
34. Nadworny PL, Wang J, Tredget EE, Burrell RE (2008) Anti-inflammatory activity of nanocrystalline silver in a porcine contact dermatitis model. Nano Nanotech Biol Med 4:241–251
35. Rogers JV, Parkinson CV, Choi YW, Speshock JL, Hussain SM (2008) A preliminary assessment of silver nanoparticles inhibition of Monkeypox virus plaque formation. Nanosca Res Lett 3:129–133
36. Gurunathan S, Lee KJ, Kalishwaralal K, Sheikpranbabu S, Vaidyanathan R, Eom SH (2009) Antiangiogenic properties of silver nanoparticles. Biomat 30:6341–6350
37. Alvarez-Salas LM, DiPaolo JA, Alvarez-Salas LM, Cipaolo JA (2007) Molecular approaches to cervical cancer therapy. Curr Drug Discov Technol 4:208–219
38. Flay LD, Matthews JHL (1995) The Effects of radiotherapy and surgery on the sexual function of women treated for cervical cancer. Int J Radiat Oncol Biol Phys 31:399–404
39. Hsin YH, Chen CF, Huang S, Shih TS, Lai PS, Chueh PJ (2008) The apoptotic effect of nanosilver is mediated by a ROS- and JNK-dependent mechanism involving the mitochondrial pathway in NIH3T 3 cells. Toxicol Lett 179:130–139
40. Compton MM (1992) A biochemical hallmark of apoptosis: internucleosomal degradation of the genome. Cancer Metastasis Rev. 11:105–119
41. Farnebo M, Bykov VJ, Wiman KG (2010) The p53 tumor suppressor: a master regulator of diverse cellular processes and therapeutic target in cancer. Biochem Biophys Res Commun 396:85–89
42. Sanchez-Perez Y, Chirino YI, Osornio-Vargas AR, Morales-Barcenas R, Gutierrez-Ruiz C, Vazquez-Lopez I, Garcia-Cuellar CM (2009) DNA damage response of A549 cells treated with particulate matter (PM10) of urban air pollutants. Cancer Lett 278: 192–200
43. Cha K, Hong HW, Choi YG, Lee MJ, Park JH, Chae HK, Ryu G, Myung H (2008) Comparison of acute responses of mice livers to short-term exposure to nanosized or micro-sized silver particles. Biotechnol Lett. 30:1893–1899
44. Ott M, Gogvadze V, Orrenius S, Zhivotovsky B (2007) Mitochondria, oxidative stress and cell eath. Apoptosis 12:913–922